NASA TECHNICAL NOTE

NASA TN D-3943

NASA TN D-3943

ASSESSMENT OF CONVECTION, CONDUCTION, AND EVAPORATION IN NUCLEATE BOILING

by Robert W. Graham and Robert C. Hendricks

Lewis Research Center
Cleveland, Ohio

NATIONAL AERONAUTICS AND SPACE ADMINISTRATION • WASHINGTON, D. C. • MAY 1967

NASA-TN-D-3943

ASSESSMENT OF CONVECTION, CONDUCTION, AND EVAPORATION IN NUCLEATE BOILING

By Robert W. Graham and Robert C. Hendricks

Lewis Research Center
Cleveland, Ohio

Technical Film Supplement C-252 available on request.

NATIONAL AERONAUTICS AND SPACE ADMINISTRATION

For sale by the Clearinghouse for Federal Scientific and Technical Information
Springfield, Virginia 22151 – CFSTI price $3.00

CONTENTS

	Page
SUMMARY	1
INTRODUCTION	1
SYMBOLS	3
DISCUSSION OF MECHANISMS	5
Bubble Agitation Mechanism	5
Vapor-Liquid Exchange Mechanism	7
Evaporative Mechanism	8
Surface Evaporation in Nucleate Boiling	11
PROPOSED MODEL OF NUCLEATE-BOILING MECHANISM	13
Boiling Surface	13
Bubble area	13
Nonboiling area	14
Heat-Transfer Mechanisms	14
Bubble-Area Mechanisms	14
Area of Preparation Mechanism	17
Nonboiling Surface Mechanism	17
General Equation for Model	18
Factors Not Considered in Model	20
Surface smoothness	20
Surface thickness and geometry	20
Thermal Diffusivity of Metal Surface	20
RESULTS AND DISCUSSION	23
SUMMARY OF RESULTS	25
APPENDIX - CALCULATION OF BOILING HEAT FLUX FROM POSTULATED MODEL	26
REFERENCES	34

ASSESSMENT OF CONVECTION, CONDUCTION, AND EVAPORATION IN NUCLEATE BOILING

by Robert W. Graham and Robert C. Hendricks

Lewis Research Center

SUMMARY

Various heat-transfer mechanisms including convection, transient conduction, and evaporation are discussed and evaluated as to their contribution to the overall nucleate-boiling heat flux. Recent boiling experiments that pertain to these mechanisms are cited. From the evaluation, a nucleate-boiling model is proposed that includes elements of each of the aforementioned mechanisms.

From a comparison of the model with experimental information on water and methanol, no single mechanism dominates over the entire boiling heat-flux range. It is true, however, that evaporation becomes the chief contributor for heat fluxes that are greater than 20 percent of the critical value.

Transient conduction is an important contributor to the total heat flux over a broad range of conditions. The cyclic removal of heat from the surface into the liquid sublayer by conduction appears to be an efficient process compared with steady-state free convection. The repeated destruction of the thermal layer that ensues the departure of a bubble enables this transient conduction process to be repeated at a bubble site.

The overall model presented herein emphasizes that nucleate boiling should be thought of primarily as a series of transient heat-transfer processes going on over distinct regions of the surface.

INTRODUCTION

Nucleate boiling is an intriguing heat-transfer process that has been the subject of numerous papers in the past two decades. Diverse models of the mechanism and the means of correlating the heat-transfer data have been presented in the literature. In fact, comparisons of some models and their associated heat-transfer correlations reveal conflicting opinions concerning the mechanisms that explain the highly efficient heat transport of nucleate boiling. Fairly detailed summarizations of the various nucleate-

boiling models and associated references are presented in references 1 to 3. However, a synopsis of the principal models appearing in the literature is presented herein for the convenience of discussion. In each of these models, one heat-transfer mechanism is considered to be dominant.

One of the earliest explanations of the mechanism of nucleate boiling suggests that the growth and departure of bubbles from a heated surface induces turbulence that promotes heat transfer between the surface and the liquid. The highly turbulent liquid transports heat into the bulk of the liquid. The bubble is a passive agent that keeps the fluid agitated but is never directly involved in the heat-transfer process. This model was the basis for several heat-transfer correlations (see ref. 4 for discussion of several correlations) that treated the heat transfer as if it were a turbulent, forced-convection process. Bubble growth rates, bubble dimensions, and bubble rise velocities were utilized as the convection elements in a Reynolds number definition, which was, in turn, a part of a Nusselt-Reynolds number correlation. Limited experimental data could be grouped by these parameters, but no universal correlation would apply to all fluids. It is interesting to observe that such Nusselt-Reynolds number correlations can be reduced to a form in which the heat flux is related to a temperature difference raised to some power (ref. 4).

A second model of nucleate boiling that was suggested pictures the bubble as a piston of a pump which displaces superheated liquid away from the surface and admits cooler liquid to the displaced region adjacent to the surface. By this cyclic process of mass transfer, large quantities of heat are transported. The originators of this model (ref. 2) claim that the high nucleate fluxes can be predicted by such an exchange mechanism. This model resembles the bubble agitation model of the previous paragraph.

A third model of nucleate boiling places emphasis on the evaporative process associated with the growth of bubbles. A correlation was developed that indicated the boiling flux to be proportional to the total volume of vapor generated (ref. 5). Other explanations of the evaporative mechanism involve a description of the evaporative interface that accounts for the vapor production. A microlayer of superheated liquid underneath the bubble was suggested by the authors of references 6 and 7. Computations presented in references 8 and 9 showed that idealized evaporative fluxes from the liquid interfaces could account for the enhanced heat transfer of nucleate boiling.

One of the objectives herein is to examine the singular roles of convection, vapor-liquid exchange, and evaporation in terms of recent experimental observations of the nucleate-boiling process. Included are heat-transfer data and visual studies of the boiling mechanism. A second objective is to postulate an overall model of nucleate boiling that includes the composite contributions of basic heat-transfer mechanisms. Postulated in several recent references are nucleate-boiling models that involve more

than one heat-transfer mechanism in the overall model (refs. 10 to 13). The model presented herein proposes time and surface area averages of the following basic heat-transfer mechanisms:

(1) Transient thermal conduction through the liquid thermal layer in the vicinity of a nucleation site that is preparing to bear a bubble

(2) Evaporation from a microlayer surface underneath a bubble that is attached to the heater surface

(3) Turbulent-free convection that is taking place over the surface areas not covered by bubbles (A zone of enhanced convection occurs in the vicinity of a growing bubble.)

Presented in this report are estimates of the various heat-transfer contributions, included in the model, for a series of boiling data in which detailed statistical information on the bubble population over a surface is available. Although several gross assumptions are involved in the calculations, the results illustrate how the several mechanisms can contribute to an overall averaged, nucleate-boiling heat flux. The reader should view these calculated results as a means of assessing the relative contribution of each mechanism on the overall heat transfer and not as another nucleate-boiling correlation.

SYMBOLS

A	area
a	coefficient of evaporation
C	constant or coefficient
c	specific heat
D_r	dry area fraction
G	mass flux
Gr	Grashof number
g_c	unit conversion from force to mass
K	enhancement factor
k	thermal conductivity
M	molecular weight
$\mathcal{M}$	dimensionless ratio
N	number of sites

n	instantaneous number of bubbles
Pr	Prandtl number
p	pressure
Q	heat rate
q	heat flux, Q/A
R	universal gas constant
r	radius
T	temperature
U	velocity
V	volumetric expansion coefficient
α	thermal diffusivity
β	contact angle
Δ	differential
δ	thickness
θ	parameter that consolidates properties for free convection
λ	heat of vaporization
μ	viscosity
ρ	density
τ	time
Φ	percent of heater area covered by both single and multiple bubbles (see table V, p. 9)
φ_m	average area under multiple bubble
$\varphi_{s,av}$	average area fraction under single bubble
$\varphi'_{s,av}$	area fraction of influence for single bubble

Subscripts:

av	average
b	bubble or bulk
calc	calculated
cond	conduction, transient
conv	convection

cr	critical
enh	enhanced
evap	evaporation
exp	experimental
gr	growth period
h	heater
l	liquid
m	mean, average or merging (bubble)
prep	preparation
r	receiver
ref	reference
s	single (bubble)
sat	saturation
v	vapor
w	waiting period or wall

DISCUSSION OF MECHANISMS

In this section, the various boiling models that have been suggested as the reasons for the large heat-transfer coefficients of nucleate boiling are discussed individually in the light of experimental evidence. Schematic diagrams of the models are shown in figure 1. The possibility of any one of these models being the dominant model in nucleate boiling is evaluated.

Bubble Agitation Mechanism

Considerable experimental evidence shows that an appreciable degree of fluid mixing occurs near the heater surface during boiling. As portrayed in figure 1(a), the presence of bubbles growing on the heater surface and departing therefrom induce this mixing or agitation process. In reference 14, schlieren and shadowgraph high-speed motion pictures were made of the thermal boundary layer in the vicinity of a bubble site. From this study, it was clear that the development of a bubble caused appreciable agitation in

the thermal layer. As the bubble grew, it appeared to displace the thermal layer, and agitation was visible within the adjacent thermal layer as far away as one bubble diameter from the center of the growing bubble. The surface area subject to this agitation is defined as the area of influence (see ref. 14).

Figure 2 presents three frames of high-speed motion pictures showing the growing bubble and the displaced surface thermal layer that extends outside the bubble. A more vivid picture of this phenomenon can be obtained by viewing the film supplement to reference 14. This area of influence of a growing bubble was observed in a different manner by Gaertner and Westwater (ref. 15), who observed the density of bubble sites across a boiling surface by having each bubble "print" its presence on the surface by a plating technique. They observed that the packing density of the bubbles produced an area of influence which was equivalent to that observed in reference 14. Apparently, the agitation destroys the thermal layer and limits the surface area that can be covered with bubbles.

The real question concerning the agitation phenomena in nucleate boiling relates to their influence on the level of the heat-transfer coefficient. Certainly, fluid oscillation or translational motion produces enhancements but are these enhancements sufficient to raise the heat-transfer coefficient by 1 or 2 orders of magnitude beyond free convection? In reference 10, Kast states that the fluid friction present would prevent the development of convective velocities of sufficient magnitude to produce heat-transfer coefficients equivalent to nucleate-boiling values. His analytical arguments were based on a forced-convection, Nusselt correlation of the boiling phenomenon. Kast cited some work wherein he measured the convective effects of bubbles in a bubble tower and observed maximum coefficients of 2000 watts per square meter per ^{o}C, which are 2 orders of magnitude below that observed with nucleate boiling. The author claimed that the bubbles left the surface in the same manner as they did in pool boiling.

In reference 16, the authors studied the pool heating of hydrogen in both its subcritical and supercritical pressure states. They observed that, in the supercritical state, a boiling-like action took place at the heating surface. Agglomerates of warm fluid rose from the surface with the appearance of bubbly vapor production. The pool appeared to be highly agitated. Nevertheless, the heat-transfer coefficients for the supercritical fluid were almost 2 orders of magnitude less than those observed for nucleate boiling. The same kind of result was noted for water (ref. 17).

Forster and Greif (ref. 2) pointed out that the bubble-agitation model would imply that the heat flux is strongly dependent on the temperature difference between the wall and bulk temperatures. Experimental evidence shows that the heat flux correlates better with $T_w - T_{sat}$ for a range of subcooling. Employing $T_w - T_b$ results in families of curves separated parametrically by the subcooling.

From the evidence cited in this section, bubble agitation does not appear to be a

singular cause of the large heat-transfer coefficient noted in nucleate boiling. The bubble-agitation mechanism can be an important contributor to the effective nucleate-boiling coefficient. The enhanced contribution of bubble agitation to a free-convection process was studied in reference 18. Gas bubbles generated by electrolysis at a heat-transfer surface (no heat of vaporization involved) produced up to fourfold enhancement in the free-convection process. The degree of enhancement was primarily dependent on the wall- to bulk-temperature difference and secondarily dependent on the electrolytic rate of gas-bubble production. The enhancement in the heat-transfer coefficient was greatest at the lower temperature differences. To maintain only free convection, the liquid (sodium hydroxide) was highly subcooled.

Vapor-Liquid Exchange Mechanism

Forster and Greif (ref. 2) proposed a model of nucleate boiling known as the vapor-liquid exchange mechanism. This model, while similar in some respects to the bubble-agitation model, was devised in response to certain objections, as discussed in the previous section.

The vapor-liquid exchange mechanism (fig. 1(b)) is a means of pumping a slug of hot liquid away from the wall and replacing it with a cooler slug. The cooler slug picks up heat from the wall before being transported out into the bulk. A growing and departing bubble acts as the piston in this pumping process. In discussing the merits of this model, Forster and Greif contended that vaporization could not explain the high heat flux associated with nucleate boiling. They argued that the enthalpy-carrying capacity of the liquid slug was the answer and formulated a ratio $\mathcal{M}$ which is the ratio of the heat capacity of a liquid slug to the latent heat content of a comparable volume of vapor. This ratio is expressed in equation form as

$$\mathcal{M} = \frac{c\rho_l}{\lambda\rho_v} \Delta T_m \tag{1}$$

where ΔT_m is the difference between film temperature and bulk temperature. Because this ratio was computed to be of the order of 10^2 from data obtained by Gunther and Kreith (ref. 19), Forster and Greif concluded that vaporization could not be important. However, serious objections can be raised as to how Forster and Greif estimated the vaporization contribution. The volume of the departing bubble was assumed to be a measure of the evaporative process, and a simultaneous evaporation-condensation process was not considered to take place within the growing bubble. They did admit such a possibility by referencing the early work of Snyder (ref. 6), which had just been

started when their paper was published. In the next section of this report, which deals with evaporative mechanisms, the work of Snyder and others is discussed.

One of the basic assumptions of the liquid-vapor-exchange calculation supposes that a volume of liquid the size of a departing bubble is at an average temperature between the wall and the bulk values. This assumption was questioned by Bankoff (ref. 1) who, in particular, was critical of assuming that the hot-liquid slug was at film temperature, which would imply a thermal-layer thickness of the order of the maximum bubble radius. Measurements of the thermal-layer thickness that were made by probing (ref. 20) and by visual techniques (ref. 21) indicate that the bubble radius is generally much larger than the thermal layer. However, shadowgraphs and schlieren photographs of the thermal layer (ref. 14) did give credence to that aspect of the model which pictured a cooler slug of liquid being heated adjacent to the hot wall. The waiting period of the ebullition cycle occurs during this process. It is important to emphasize that the liquid being heated was within the thermal layer and that it was a thin layer of liquid that heated cyclicly during ebullition. In reference 22, Hsu pictured the development of the thermal layer in the vicinity of a bubble site as a prerequisite to bubble incipience. In his analysis, the thermal layer was treated as a semiinfinite slab undergoing transient conduction.

Summarizing the discussion of the vapor-liquid exchange mechanism, it has been shown that there is experimental proof that such a mechanism exists physically. It is doubtful that its potential heat-flux contribution was correctly computed in reference 2 for the reasons cited previously. The mechanism is probably significant in replenishing the thermal layer with cold liquid after a bubble departs.

Evaporative Mechanism

Any explanation of nucleate boiling must be capable of explaining the abrupt enhancement in heat transfer observed when boiling begins. The two models discussed thus far (bubble agitation and vapor-liquid exchange) have proposed such an explanation in terms of the intensification of free-convection processes that are in effect at heat fluxes below the boiling incipience value. A third explanation is that the abrupt change in the boiling-heating curve is attributable to evaporation.

Evaporation from a free liquid surface can be considered as an effusive molecular flow (ref. 23) and thus can be treated as a problem in the kinetic behavior of a gas or a vapor. In this section, the rate equation for evaporation is reviewed, and numerical estimates of heat-flux values possible from evaporating surfaces are presented.

Consider a free liquid surface at saturation conditions and above the liquid a blanket of vapor of the same substance as the liquid. This vapor is also at saturation condi-

tions. A kinetic equilibrium exists whereby a certain rate of evaporating molecules from the liquid will be replaced by an equal rate of condensing molecules from the vapor. From kinetic theory, the mass rate of molecules involved in this evaporation-condensation exchange is given by

$$G = \left(\frac{2\pi RT_{sat}}{g_c M}\right)^{-1/2} p_l \tag{2a}$$

In a real boiling process in which a net production of vapor is involved, the aforementioned kinetic equilibrium is upset by a temperature or pressure difference, which lowers the pressure in the vapor with respect to the liquid pressure. If the vapor is at some receiver pressure p_r, the net evaporation rate is given by the following equation, which is a modification of equation (2a):

$$G_{evap} = \left(\frac{2\pi RT_{sat}}{g_c M}\right)^{-1/2} (p_l - p_r) \tag{2b}$$

It has been observed experimentally that this rate equation is correct for atomic or molecular structures that exhibit geometric symmetry, but comparatively complex molecules like water or long-chain hydrocarbons exhibit evaporation rates that are a small fraction of those predicted by equation (2b). The ratio of the measured to the theoretical evaporation rate is defined as the evaporation coefficient a. Wyllie (ref. 24) measured the coefficients of evaporation for several fluids, some of which are given in table I. These coefficients were obtained by measuring the mass flow through a diffusion hole into a hard vacuum system and by comparing the experimental result with evaporation rates predicted from equation (2b) (with the receiver pressure equal to zero). Wyllie (ref. 24) envisioned a three-layer model of the evaporation mechanism. First was the liquid substrate with a compact, ordered layer of liquid molecules. Above that was a mobile absorbing layer of molecules. On top of the mobile layer was the vapor. For a high coefficient of evaporation, the rate of exchange between the liquid substrate and the mobile layer must be much greater than that from the mobile layer into the vapor. It is inter-

TABLE I. - COEFFICIENTS OF EVAPORATION (REF. 24)

Fluid	Coefficient of evaporation, a
Carbon tetrachloride (CCl_4)	1
Benzene (C_6H_6	.90
Chloroform ($CHCl_3$)	.16
Ethanol (C_2H_5OH)	.02
Methanol (CH_3OH)	.045
Water (H_2O)	.040

esting to observe (as was pointed out in ref. 24) that those fluid molecules with large dipole moments had lower rates of evaporation. For example, carbon tetrachloride (CCl_4) with a zero dipole moment had an evaporative coefficient of 1, whereas water with a dipole moment of 1.85 had an evaporative coefficient of only 0.04. Other values of evaporative coefficients appear to correlate (inversely) with the magnitude of the dipole moment. Reference 25 presents a more recent compilation of evaporative coefficients and an excellent review of the topic. Refined experiments for several fluids made by Eagleton and his colleagues (refs. 26 and 27) corroborate the general magnitude of the values published in reference 24.

In several papers, the mass transfer and heat removal during surface evaporation was computed from the kinetic theory. Plesset (ref. 8) computed the net flux of vapor being transported from a hot, liquid interface to a cooler, liquid surface. The Plesset equation included a condensation coefficient as an unknown, which could be computed by the use of the equation. Usually, for equilibrium evaporation, the condensing coefficient is assumed to be equal to the evaporative; but for nonequilibrium situations, this need not be true.

Bankoff (ref. 9) made use of reference 8 to show that the upper limit of nucleate boiling for several hydrocarbons was predictable as an evaporative-condensing process.

It is interesting to examine the theroetical heat-transfer rate that is possible through evaporation of a fluid into a receiver. When the heat of vaporization is taken into account, equation (2b) can be modified to express the flux of heat leaving the surface. The coefficient of evaporation a is included in the equation:

$$q = a\lambda\left(\frac{2\pi RT_{sat}}{g_c M}\right)^{-1/2}(p_l - p_r) \tag{2c}$$

TABLE II. - THEORETICAL EVAPORATIVE HEAT-FLUX RATES

[Saturation pressure, 1 atm.]

Fluid	Saturation temperature, T_{sat}, ^{o}R	Heat of vaporization, λ, Btu/lb mass	Molecular weight, M	Coefficient of evaporation, a	Evaporative heat flux	
					Btu/(hr)(ft^2)	W/m^2
Mercury	1135	126	200.6	1	44.4×10^6	140×10^6
Water	672	970	18	.04	2.78	8.8
Ethanol	632	363	46.1	.02	.85	2.7
Methanol	608	473	37.0	.045	2.1	6.6
Nitrogen	139	86	28.0	1	4.7	14.8
Hydrogen	36	190	2	1	20.4	64.5

Equation (2c) was employed in computing the rates of heat transfer for mercury, water, ethyl alcohol, liquid nitrogen, and liquid hydrogen. These rates are compared in table II at a saturation pressure of 1 atmosphere and with the vapor being drawn into a perfect vacuum ($p_r = 0$). The results in the table are highly idealized and represent the case of a steady-state evaporation into a vacuum reservoir. This case is not representative of a nucleate boiling process where (1) the process is not steady, (2) the receiver pressure is not a vacuum, and (3) evaporation does not occur over the entire heating surface simultaneously. Nevertheless, table II does show that evaporation is a highly efficient heat-transfer mechanism that can be 2 orders of magnitude greater than liquid-free convection. Consequently, the presence of evaporation over only a small portion of a heat-transfer surface at any one time could increase the overall heat-transfer rate, which could be the explanation of the almost discontinuous jump in heat transfer noticed when nucleate boiling begins.

Surface Evaporation in Nucleate Boiling

The evaporative mechanism has been demonstrated analytically to account for sizeable heat-flux rates. The problem of showing experimentally that a surface-evaporation phenomenon is present with nucleate boiling, remains. A number of independent investigators (refs. 3, 7, and 28 to 30) noted appreciable diminution of local wall temperatures underneath a bubble during the growth period. Figure 3 (from ref. 3) graphically illustrates this observation. The figure includes the transient surface-temperature history underneath a bubble and a computed curve of the transient heat flux during the ebullition cycle. High-speed motion pictures of the bubble history show the condition of the bubble at various times in the transient. The heat-flux curve points to the importance of the comparatively short interval of rapid bubble growth in contributing to the overall heat flux. As indicated by the temperature curve of figure 3, the severe drop in local wall temperature during bubble growth appears to contradict the liquid-vapor-exchange concept, which presumes that surface cooling would not start until after the bubble (or bubbles) departed and quenching had begun. It also contradicts a presumption of the bubble stirring, or agitation model, which would envision appreciable cooling of the local surface underneath a bubble because of induced turbulence as cooler liquid replaces the bubble volume.

Estimates of the heat-transfer rate during bubble growth are presented in reference 3. With water as the fluid, at somewhat subcooled conditions, the heat-transfer rates were as high as 500 000 Btu per hour per square foot (1 580 000 W/m^2). This maximum value approaches the magnitude of the idealized heat flux predicted from the kinetic theory of evaporation (see table II, p. 9). Mason and Bankoff (ref. 31) reported

values of heat-transfer coefficient at a surface where rapidly growing and collapsing bubbles were present. These coefficients ranged in magnitude from 13 000 to 300 000 Btu per hour per square foot per ^{o}F (74 000 to 1 700 000 $W/(m^2)(^{o}C)$). Such a range of heat-transfer coefficient could produce heat-flux rates comparable to, or even an order of magnitude higher than, those reported in reference 3. Direct comparison between references 3 and 31 cannot be made because the fluid-state conditions were not comparable.

The inclusion of the concept of an evaporative mechanism at the base of a bubble necessitates the presence of a thin liquid layer there. Such an assumption was made by Snyder and Edwards (ref. 6) and also by Moore and Mesler (ref. 7) in proposing the presence of a microlayer of liquid underneath the bubble. Experimental verification of the presence of the microlayer has been established by at least two independent investigations. Hospeti and Mesler (ref. 32) used a chemical deposition technique involving calcium sulfate which contained radioactive sulfur 35. The radioactive sulfur made possible the measurement of the amount of deposit residue left by a sequential history of many bubbles developing at a particular site. Autoradiographs of the deposits could be related to the amount of liquid boiled off in generating the bubbles; thus, estimates of the thickness of the liquid microlayer under the bubble could be made. For average heat fluxes ranging from 7000 to 20 000 Btu per hour per square foot (22 000 to 63 000 W/m^2), the microlayer thickness was observed to vary from 19×10^{-6} to 10^{-4} inch (4.84×10^{-7} to 2.54×10^{-6} m).

Sharp (ref. 33) employed three kinds of experimental techniques to detect the presence and magnitude of the microlayer.[1] The simpler of the techniques was the use of an electrical continuity probe that was inserted into the base of a growing bubble. The indication of electrical continuity between the probe and the heating surface was interpreted as the presence of a thin liquid layer. The more sophisticated method involved the application of the optical principles of interference fringes (Newton's rings) to measure the thin microlayer. Sharp was able to make estimates of the local thickness of the microlayer at various radial positions beneath the bubble at several time intervals of bubble growth. Curves of microlayer thickness from reference 33 are reproduced in figure 4. It is apparent that the measured microlayer thickness varied between 1000 and 4000 Å, or approximately 4×10^{-6} to 16×10^{-6} inch (1.02×10^{-7} to 4.06×10^{-7} m). These values are somewhat smaller than those observed by Hospeti and Mesler (ref. 32), but it is remarkable that there is an overlapping range of general agreement. Sharp used the measured values of the depletion rate of the microlayer to predict an average heat-flux rate underneath the bubble. The average rates varied between 30 000 and 50 000 Btu per hour per square foot (95 000 to 158 000 W/m^2) for the area under the bubble.

[1] A NASA-Lewis motion picture (C-252) describing the experimental methods and including film clips from the research sequences is available on loan. A request card and description of the film are included at the back of the report.

PROPOSED MODEL OF NUCLEATE-BOILING MECHANISM

As a result of the evaluation of a number of mechanisms of nucleate boiling presented in the previous sections, the following overall model of the nucleate boiling cycle was constructed. This proposal incorporates specific features from the several models that appear to agree with recent experimental evidence.

Boiling Surface

Bubble area. - A boiling surface such as that depicted in figure 5(a) contains N number of boiling sites that are active at a given heat flux. Instantaneously, there are bubbles, which can be single, or multiple, over a certain fraction of these sites. For an intermediate range of nucleate-boiling heat flux, both single bubbles and multiple bubbles that consist of several single bubbles may occur simultaneously. A statistical number of all the instantaneous bubbles (in single and multiple form) is designated as n_{av}. The size of the bubbles appearing on this surface will vary from site to site, and the size of each individual bubble will vary during the growth period; nevertheless, a statistical bubble, which represents an average size of a typical bubble growing on the surface, can be envisioned. Such statistical information can be obtained by tediously examining high-speed motion pictures of boiling on a surface. An instantaneous statistical picture of the fraction of the surface covered by vapor can be determined.

For the model presented herein, the projected surface area underneath the bubbles is of primary interest. The general bubble shape is assumed to be that of a truncated sphere; thus, the contact surface area between the bubble and the surface may vary anywhere from a circle of the bubble radius r_b (hemispherical bubble) to a circle of only a fraction of the bubble radius. It is assumed that the large multiple bubbles can also be represented by this geometry.

A profile view of three statistical bubbles ($n_{av} = 3$) on the surface is presented in figure 5(b). The average contact area of the bubbles can be related to a contact angle β, defined in the figure. This contact angle is often associated with the liquid contact angle measured on the meniscus of capillary tubes. Although the bubble contact angle and the liquid contact angle may be related, they are not identical. Measurements of bubble contact angles appear in the literature. References 34 and 35 show that the contact angle of a bubble varies during the growth time. For the model presented herein, a value of β averaged over the growth period of a bubble is used, and isolated bubble values for β are applied to the multiple bubbles.

Figure 5(a) shows phantom drawings of areas that will eventually be populated with bubbles. These areas were drawn equivalent to the projected bubble area A_b. The

thermal layer is being conditioned during a waiting period for the generation of new bubbles. The ratio of the statistical area of growing bubbles to the area in preparation is a function of the ratio of the growth to the waiting periods. If the waiting period is longer than the growth period, more surface area of preparation than area of growing bubbles is present instantaneously. The relative distribution of the bubble and preparation areas is reversed when the growth period is greater than the waiting period. (In fig. 5, the waiting period is twice the growth period.) At higher heat fluxes, more sites would become active.

Nonboiling area. - The area of the surface (fig. 5(a)) that is outside the solid line, or phantom areas shown, is considered a nonboiling area. This area of nonboiling may be appreciably large at low values of the average boiling heat flux and will probably disappear at heat fluxes corresponding to the critical or burnout value.

Heat-Transfer Mechanisms

In the previous section, a boiling heat-transfer surface was divided into (1) a projected surface underneath a growing bubble, (2) a surface where the thermal layer is being prepared for ebullition, and (3) a surface where no boiling activity takes place. The heat-transfer mechanisms in process over each of these areas are discussed, which necessitates subdividing these areas further (shown in fig. 5(a)) for the specific mechanisms involved. A pictorial description of the various heat-transfer mechanisms that make up the overall heat transfer is presented in figure 6. Essentially, this is figure 5 modified to illustrate where the various heat-transfer mechanisms are in effect.

Bubble-Area Mechanisms

As shown in figure 6, the form of the bubble over this area is assumed to be a truncated sphere. The surface area in contact with the bubble is assumed to be wetted, with the exception of a possible dry spot that develops during the bubble lifetime. The growth of the dry spot is discussed in reference 33. The behavior of the dry spot is discussed more fully in the appendix. Limited evidence indicates that the dry fraction of the bubble contact area remains constant over a broad span of the nucleate heat flux. As the heat flux approaches the critical, or burnout, condition, the fraction of dry area to total area asymptotically approaches 1 (see fig. 7). The heat-transfer mechanism above the dry spot is assumed to be gaseous convection, and the heat-transfer contribution is negligibly small.

The wetted contact area is considered to be a microlayer (see refs. 32 and 33) that is the evaporative surface for the supply of vapor into the bubble. Kinetic theory from an evaporative surface is employed to compute the local heat transfer.

Questions arise regarding the legitimacy of applying the kinetic theory expression to the evaporative process on a microlayer surface. Generally, the picture of static conditions and thermal equilibrium at the vapor-liquid interface pertains to the kinetic equation, but this is not the case for the microlayer in a bubble environment. Presumably, the microlayer is being supplied fresh liquid during the growth period, and the vapor inside the bubble is highly agitated, which results in rather dynamic, nonequilibrium conditions at the liquid interface. However, the velocities of the molecular species participating in the phase change are several orders greater than the macroscopic fluid velocities of the bubble interior or of the microlayer. Thus, the application of equation (2c) to the microlayer may be a good approximation of the evaporative process occurring there.

The wetted, or evaporative, area (from fig. 6) can be described as

$$A_{evap} = n_{av}\pi r_b^2(1 - D_r)\sin^2 \beta \tag{3}$$

where D_r is the dry faction of the bubble contact surface. When equation (2c) is used, the heat transfer from the wetted surface is

$$Q_{evap} = a\lambda(p_l - p_r)\left(\frac{g_c M}{2\pi R T_{sat}}\right)^{1/2} A_{evap} \tag{4}$$

For isolated bubbles, when the bubble contact angle is less than 90^o, an annulus is present underneath the projected bubble area that is not a part of the wetted area. This part of the projected bubble area and an annular area outside the projected bubble area (see fig. 6) are assumed to be areas of enhanced free convection. As observed in reference 10, this enhanced region outside the bubble appeared to extend one bubble diameter away from the center of the bubble. The enhanced free convection is greater than the turbulent-free convection computed for a horizontal flat plate. Thus, a factor K is introduced to enhance the computed free-convection value, which applies to the convection region under the bubble (if it exists) and the area of influence. For ordinary turbulent free convection, the equation applicable to horizontal surfaces is

$$q = C(GrPr)^{1/3}\frac{k}{\delta}(T_w - T_b) \tag{5a}$$

where

C empirical coefficient for ordinary free convection

Gr Grashof number, $V\delta^3(T_w - T_b)g\rho^2/\mu^2$

g local acceleration of gravity

δ characteristic thickness

Pr Prandtl number

Noting that the characteristic thickness δ cancels out and collecting similar terms yield

$$q_{conv} = C\left(\frac{Vg\rho^2}{\mu} ck^2\right)^{1/3} (T_w - T_b)^{4/3} \tag{5b}$$

Grouping the coefficient C and the fluid property term produces the simple empirical equation

$$q_{conv} = \theta(T_w - T_b)^{4/3} \tag{5c}$$

where

$$\theta = C\left(\frac{Vg\rho^2}{\mu} ck^2\right)^{1/3}$$

For turbulent free convection on horizontal surfaces, data are available, and the value of θ can be determined. Thus, the heat-transfer contribution for the surface involved in enhanced convection is

$$Q = Kq_{conv}n_{av}\pi r_b^2(4 - \sin^2 \beta) \tag{6}$$

The selection of a value for the factor K is a problem. The average effects of superposing bubbling on a free-convection process were considered in reference 18. Electrolytically generated bubbles produced enhancement ratios that ranged from slightly greater than 1 to as high as 4. The latter value occurred at the lower temperature differences, and, consequently, may reflect changes in the free-convection mechanism from a laminar to a turbulent free convection. With boiling present, a laminar-type free convection does not seem likely; thus, the enhancement ascribed to bubbling would be more comparable to what the authors of reference 18 saw at higher temperature differences, where the maximum enhancement ratio was approximately 2. As an average representative value of enhancement, 1.5 would be a reasonable approximation. Consequently, a constant factor of 1.5 is the multiplier K of equation (6) to account for

the enhanced convection ascribed to bubble-growth effects. This value is assumed to apply to all fluids, although it should be a variable and account for the different rates of bubble growth, the size of bubbles, and the density of bubble sites - to mention a few influences. Because no direct way of accounting for these variations is apparent, the enhancement factor is considered to be a constant in the model proposed herein.

Area of Preparation Mechanism

Shown in figure 6 are areas where the thermal layer was making a transition to a condition that would produce ebullition. As discussed in reference 22, this period of transition, commonly known as the waiting period, can be approximated as a transient conduction process into a semiinfinite fluid slab. The equation for transient conduction is well known. The length of time involved in the transient conduction is taken as the waiting period τ_w, and the contribution from the area of preparation is

$$Q_{cond} = 2k\sqrt{\frac{1}{\pi\alpha\tau_w}}(T_w - T_b)A_{prep} \tag{7}$$

The area of preparation A_{prep} is $n_{av}(\tau_w/\tau_{gr})\pi r_b^2$. It was mentioned earlier that, if all the sites could be typified by one identical type, the ratio of the preparation areas to the growth areas would be proportional to the ratio of the waiting to the growth periods. At the higher nucleate heat fluxes, a situation will arise in which the areas of preparation will overlap the area of evaporation. This situation is discussed in detail in the appendix. The temperature difference for the waiting period was assumed to be between that of the wall temperature and the bulk conditions in the liquid.

Nonboiling Surface Mechanism

The nonboiling surface constitutes the area remaining on the surface that is not involved directly in any aspect of the ebullition process. The mechanism of heat transfer is turbulent free convection. Equation 5(c) describes this process. The area involved in the free-convection process is

$$A_{conv} = A_h - A_{evap} - A_{enh\ conv} - A_{prep} - A_d$$

$$= A_h - n_{av}\pi r_b^2(1 - Dr)\sin^2\beta - n_{av}\pi r_b^2(4 - \sin^2\beta) - n_{av}\pi r_b^2 \frac{\tau_w}{\tau_{gr}} - n_{av}\pi r_b^2\, Dr \sin^2\beta \quad (8)$$

$$Q_{conv} = \theta(T_w - T_b)^{4/3}\left[A_h - n_{av}\pi r_b^2\left(4 + \frac{\tau_w}{\tau_{gr}}\right)\right] \quad (9)$$

General Equation for Model

An equation for all the heat-transfer mechanisms in process at any instant over the entire surface is simply the sum of all the contributions for each of the subareas. When this equation is written as a heat flux q_{av}, it is expressed as follows:

$$\frac{Q}{A_h} = q_{av} = \left[\frac{n_{av}\pi r_b^2}{A_h}(1 - Dr)\sin^2\beta\right]\left[a\lambda(p_l - p_r)\left(\frac{g_c M}{2\pi RT}\right)^{1/2}\right]$$

$$+ \left[\frac{n_{av}\pi r_b^2}{A_h}(4 - \sin^2\beta)\right] K\theta(T_w - T_b)^{4/3}$$

$$+ \left(\frac{n_{av}\pi r_b^2}{A_h}\frac{\tau_w}{\tau_{gr}}\right)\left[2k\frac{1}{\sqrt{\pi\alpha\tau_w}}(T_w - T_b)\right]$$

$$+ \left[1 - \frac{n_{av}\pi r_b^2}{A_h}\left(4 + \frac{\tau_w}{\tau_{gr}}\right)\right]\theta(T_w - T_b)^{4/3} \quad (10a)$$

In the actual calculation procedure, it was convenient to use equation (10a) in the following form:

$$q_{av} = \left[\Phi(1 - Dr)\sin^2\beta\right]q_{evap} + \left[\Phi(4 - \sin^2\beta)\right]Kq_{conv}$$

$$+ \Phi\frac{\tau_w}{\tau_{gr}}q_{cond} + \left[1 - \Phi\left(4 + \frac{\tau_w}{\tau_{gr}}\right)\right]q_{conv} \qquad (10b)$$

The application of equation (10a) to compute an average overall heat flux requires considerable experimental input information about the particular boiling condition in question. Statistical information on the amount of surface area covered by bubbles and the relative magnitudes of the growth and waiting periods is required. Surface and bulk temperature data are also needed. Thus, the model proposed herein cannot be considered to be a prediction technique, which would be capable of predicting the fraction of surface area covered by bubbles and the relative magnitudes of the growth and waiting periods. Predicting this area is a difficult task that requires more detailed information than is presently known about the formation and growth of bubbles. Further studies are needed on the evaporation, condensing, and convection processes associated with establishing bubble size. Vapor appearing in a bubble is speculated to be the instantaneous surplus of vapor not condensed over the bubble cap. If this is true, bubble size could be predicted from information about the efficiency of evaporation and condensing rates over the bubble surface.

Equation (10a) was developed as a means to compute the relative contributions of several heat-transfer mechanisms considered to be important in the overall nucleate-boiling heat transfer. Such a calculation will lead to an assessment of the relative importance of the heat-transfer mechanisms for a known nucleate-boiling condition.

The appendix contains calculations made by employing equation (10a) for nucleate-boiling data in which temperature data and statistical information on the fraction of the surface covered by single or multiple bubbles were available. Water and methanol were the fluids used in the comparison between the computed and measured heat fluxes.

References 11 and 36 were used to obtain heat flux and temperature data for water. Reference 37 was used to obtain heat flux-temperature information for methanol. Reference 38 provided information on the average bubble population (single and multiple bubbles) and on the average surface area covered by these bubbles (for both water and methanol). These data were obtained from a careful examination of high-speed motion pictures and represent a statistical analysis of many data samples. Reference 38 presents information on the average heat-flux and bulk-fluid conditions but gives no surface-temperature data. Reference 39 contained near-burnout data for water.

Factors Not Considered in Model

Since the proposed model involves transient processes near the liquid-solid interface, the smoothness of the solid surface, its thickness, and the thermal diffusivity of the material will be influential. Such effects are not included in the equations for the model presented herein.

Surface smoothness. - Numerous observations have been made which show that nucleation is strongly related to the surface smoothness. Hsu (ref. 22) demonstrated that the thermal conditions (thermal-layer profile and thickness) for a nucleation criterion can be related to the dimensions of a scratch or pit. However, no one has been able to present a general correlation for bubble population, frequency, and surface distribution as a function of surface roughness. Thus, an accounting for the surface cannot be included in the model presented herein.

Surface thickness and geometry. - Experimental boiling data that cover a variety of heater geometries, including wires, thin ribbons, rods, tubes and thick blocks are presented in the literature. These heater geometries can influence the surface-temperature distributions and the transport of heat into the fluid. For example, a thin metal ribbon would differ significantly from a thick block of the same material in that the block would be apt to provide a constant surface temperature and a variable instantaneous heat flux, whereas the thin ribbon would approximate a constant heat flux with a variable surface temperature.

Thermal Diffusivity of Metal Surface

Thermal balance across the solid-liquid interface is influenced by both the transient and steady modes of transport within the metal heater. The transient effect is discussed in reference 33, where it is shown that the transient thermal transmissivity of a finite plate is a function of $k/\sqrt{\alpha}$. This parameter was computed to range from 0.03 calories per cubic centimeter per ^{o}C for Inconel and glass to 0.09 calorie per cubic centimeter per ^{o}C for copper. Thus, copper will maintain a more constant surface temperature than glass or Inconel. The heat that is transported into the fluid at the bubble area is influenced by the thermal diffusion of the heater (ref. 6). Consequently, the diffusion properties of the heater surface are important during transient conduction into the bubble thermal layer.

TABLE III. - BASIC EXPERIMENTAL INFORMATION FROM REFERENCE 36

[Burnout heat flux for water, 5×10^5 Btu/(hr)(ft^2) (1.6×10^6 W/m^2); for methanol, 1.7×10^5 Btu/(hr)(ft^2) (5.4×10^5 W/m^2).]

Fluid	Bulk temperature, T_b, ^oF	Subcooling, ^oF	Number of frames	Number of single bubbles, n	Area fraction of influence for single bubble, $\varphi'_{s,av}$	Average area fraction under single bubble, $\varphi_{s,av}$	Average area under multiple bubble, φ_m	Sum of single and multiple bubble area fractions, $\Phi = \frac{n_{av}\pi r_b^2}{A_h}$	Instantaneous number of bubbles, n_{av}	Number of sites, N	Ratio of growth period to total period, $\frac{\tau_{gr}}{\tau_{gr}+\tau_w} = \frac{n_{av}}{N}$	Ratio of waiting period to total period, $\frac{\tau_w}{\tau_{gr}+\tau_w} = 1 - \frac{n_{av}}{N}$	Wall to bulk temperature, difference, $T_w - T_b$	Critical heat flux, q_{cr}, percent
Water	201	11	101	128	0.121	0.038	0.045	0.083	2.1	13	0.16	0.84	24	4
	198	14	102	172	.109	.046	.024	.070	2.2	15	.15	.85	28	6.5
	199	13	99	268	.138	.093	.040	.133	3.3	18	.18	.82	31	9.5
Methanol	132	16	96	328	0.127	0.108	0.038	0.146	4	18	0.22	0.78	73	28
	139	9	50	92	.167	.077	.535	.612	9.3	30	.31	.69	73	79
	111	37	70	263	.103	.097	.110	.207	6.5	20	.32	.68	97	40

TABLE IV. - COMPARISON OF COMPUTED WITH EXPERIMENTAL VALUES OF HEAT FLUX FOR WATER AND METHANOL

[To obtain heat flux in units of W/m^2, multiply numbers in table by 3.152.]

Fluid	Run	Heat flux, q, Btu/(hr)(ft^2)									
		Time averaged[a]				Time and area averaged[b]				Calculated	Experimental
		Evaporation	Transient conduction	Enhanced convection	Free convection	Evaporation	Transient conduction	Enhanced convection	Free convection		(c)
Water	1	400 000	35 700	16 500	11 000	7 050	15 500	5100	2600	30 200	21 150
	2	510 000	40 000	20 000	13 400	7 600	16 400	5200	4200	33 400	32 000
	3	514 000	52 000	23 400	15 600	15 000	31 000	8800	----	54 800	49 500
Methanol	4	1 500 000	49 400	15 000	10 000	21 900	25 000	7100	----	54 000	48 300
	5	1 860 000	80 000	18 000	12 000	94 800	75 900	----	----	170 700	135 000
	6	1 790 000	92 400	16 500	11 000	36 800	39 700	9100	----	85 600	68 400

[a]Denotes average over parts of cycle (or time interval) in which particular mechanism is working.

[b]Denotes average over time interval and over dimensionless area involved in particular heat-transfer mechanism.

[c]Data from ref. 38.

TABLE V. - COMPARISON OF COMPUTED WITH EXPERIMENTAL VALUES OF HEAT FLUX FOR WATER NEAR-BURNOUT CONDITION[a]

To obtain heat flux in units of W/m^2, multiply numbers in table by 3.152.

Input				Heat flux, q, Btu/(hr)(ft^2)									
				Time averaged[b]				Time and area averaged[c]				Calculated	Experimental
Contact area fraction	Subcooling	$T_w - T_{sat}$, ^oF	τ_w/τ_{gr}	Evaporation	Transient conduction	Enhanced convection	Free convection	Evaporation	Transient conduction	Enhanced convection	Free convection		(a)
0.5	11° F	32	1.0	1×10^6	1.67×10^5	21×10^3	11×10^3	504 000	83 500	----	----	587 500	541 000
.3	11° F	29	2.33	0.9×10^6	1.28×10^5	18×10^3	12×10^3	271 000	89 700	----	----	360 700	313 000
0.65	Saturation	31	0.54	0.97×10^6	1.21×10^5	21×10^3	14×10^3	631 000	42 300	----	----	673 300	428 000
.3	Saturation	24	2.33	$.73\times10^6$	$.68\times10^5$	18×10^3	12×10^3	219 000	47 500	----	----	266 500	170 000

[a]Data from ref. 39.

[b]Denotes average over time interval and over dimensionless area involved in particular heat-transfer mechanism.

[c]Denotes average over time interval and over dimensionless area involved in particular heat-transfer mechanism.

RESULTS AND DISCUSSION

The model of the nucleate-boiling mechanism described herein was utilized in a calculation of the various components of heat transfer that were assumed to be involved in the overall nucleate-boiling process. The input data employed in the calculations are given in table III. As mentioned in the section Description of Model, the assumptions and approximations related to the use of these data are part of the appendix.

The results of the calculation are presented in table IV. The contribution of each heat-transfer mechanism is tabulated along with the overall average heat flux. The final column in the table presents the experimental average heat flux from reference 38. Note that the tabulations include computed time-averaged values and values where both time and heat-transfer surface weighting are involved. The dashes in the table signify that area overlapping of mechanisms associated with the ebullition process appropriated the entire surface and left no areas for convection. The procedure used for this situation in the calculation is discussed in the appendix.

At first glance, the comparison of experiment with analysis in table III may seem limited in terms of the number of comparisons. However, it should be realized that the source of information on the bubble areas, the average growth and waiting periods, the number of bubbles, etc. used in the comparison represents an exhaustive statistical study of hundreds of bubbles (ref. 38). Realistically, these six runs should be considered as representative of scores of nucleate-boiling data points.

The last two columns of table IV do show remarkable agreement in the computed overall heat flux and the experimental values. It should be noted that the calculations for water represent relatively low heat fluxes with respect to critical or burnout heat flux. Information on the surface area involved in the merging bubbles for water could not be discerned easily; consequently, reference 38 did not contain information relevent to near-critical heat fluxes of water. Reference 39, however, did present instantaneous measurements of the bubble contact area over a range of fluxes including the critical value. No data were presented on the number of sites, the merging of bubbles, or the bubble frequency. The ratio of bubble growth to waiting time was computed by assuming that

$$\frac{\tau_w}{\tau_{gr}} = \frac{A_{prep}}{A_{evap}} \tag{11}$$

subject to the constraint that $(A_{prep} + A_{evap})/A_h \leq 1$ (see appendix for further discussion). These near-burnout comparisons for water (based on ref. 39) are tabulated separately in table V for two heat-flux levels at saturated and subcooled conditions. Again, the

computed results agree reasonably well with the experimental measurement. For some unknown reason, the agreement is better for the subcooled cases.

The stated objective of this report was to present a balanced observation of the relative contributions of several mechanisms that are thought to make up the overall nucleate-boiling heat flux over a range of heat fluxes. In figure 8, the relative contribution of each heat-flux component is plotted as a function of the percent of critical heat flux. An examination of the figures leads to the following observations:

(1) For both water and methanol, no single mechanism dominates over the entire boiling heat-flux range. It is true, however, that evaporation becomes the chief contributor for heat fluxes that are greater than 20 percent of the critical value. The well-known hydrodynamic-instability, critical-heat-flux models of Zuber and Kutateladze (see ref. 40) indicate that evaporation is the dominant heat-transfer mechanism near the critical heat flux. In their model, the critical heat flux develops when the hydrodynamic instability limits the amount of heat-transfer surface wetted by the liquid phase. In the analytical expression, the critical flux is directly proportional to the heat of vaporization.

(2) The relative contribution of the evaporation mechanism is higher with water than with methanol. Since water does have a much higher heat of vaporization than methyl alcohol, this trend would be expected.

(3) Transient conduction is an important contributor to the total heat flux over a broad range of conditions. The cyclic removal of heat from the surface into the liquid sublayer by conductions appears to be a very efficient process compared with steady-state free convection. The repeated destruction of the thermal layer that ensues the departure of a bubble enables this transient-conduction process to be repeated at a bubble site.

The overall model presented herein emphasizes that nucleate boiling should be thought of primarily as a series of transient heat-transfer processes over distinct regions of the surface. The computation of an average heat flux requires knowledge of the time and spacial averaging of the heat-transfer processes.

Considerable experimental information is still needed to give more comprehensive information on aspects of the nucleate-boiling mechanisms over a range of heat flux and subcooling. The limited amount of information on the bubble contact area needs to be expanded. The behavior of the microlayer and the dry spot should be studied at higher heat fluxes. The distribution of condensing and evaporating heat-transfer coefficients over a bubble surface requires study. The diffusion of the thermal energy into the fluid bulk is another subject that deserves some attention for better overall understanding. The model discussed herein treats the heat transport across a fluid resistance at the interface between the surface and the fluid. The means for absorbing that thermal energy in the bulk is not considered. In two-phase flow processes, the mechanism of thermal-energy absorption in the bulk is particularly important. The void distribution

across the channel and the enthalpy gradients in both the radial and axial directions are related to it.

Mention was made earlier of the effect of the surface condition and the surface material on the overall boiling process. The limited experimental information on this subject suggests that this topic be further pursued.

In this discussion, several obvious deficiencies in experimental information on nucleate boiling were cited. The list is by no means complete. Even a partial listing gives emphasis to needed research in nucleate boiling.

SUMMARY OF RESULTS

1. An overall model of nucleate boiling, based on recent experimental observations by several investigators, is presented. The model incorporates convection, transient conduction, and evaporation - heat-transfer mechanisms. The contribution of each mechanism is weighted according to spacial and time averaging.

2. Statistical experimental data for water and methanol were used as input to the heat flux equations of the model. The resulting computed overall heat fluxes agreed well with experimental results over a wide range of heat flux.

3. No one single mechanism dominates over the entire range of overall nucleate-boiling heat flux. Evaporation is the major contributor when the heat flux is greater than 20 percent of the critical or burnout value. Transient conduction is next in importance.

4. The use of the analytical model emphasizes the need for more basic information on aspects of nucleate boiling over a range of heat flux and subcooling. Studies on bubble contact area, evaporative-condensing processes in bubbles, and thermal diffusion into the liquid bulk would make possible predictions of the input information needed for the model. Such generalized information may transform the model from just an analytical description of nucleate boiling into a prediction technique.

Lewis Research Center,
National Aeronautics and Space Administration,
Cleveland, Ohio, January 5, 1967,
129-01-09-04-22.

APPENDIX - CALCULATION OF BOILING HEAT FLUX FROM POSTULATED MODEL

It was pointed out previously that experimental information is needed to compute the average boiling heat flux from equation (10a). The model presented herein will not predict the surface conditions. Experimental information from references 11 and 36 to 38 is employed to compute heat flux for water and methanol. This input information is given in table III. In addition to the assumptions and approximations included in the model description, certain other assumptions and approximations are employed in the calculation that are explained in this appendix. Some repetition of the assumptions mentioned previously are necessary. A sample calculation appears at the end of this appendix. The various heat-transfer mechanisms associated with the division of areas shown in figure 6 are discussed separately.

Evaporative Area Under Bubble

Dry area. - As depicted in figure 6, the evaporative area is the base of the truncated spherical bubble minus the dry-spot area. The fraction of the bubble contact surface that was dry was assumed to be a function of the magnitude of the average boiling heat flux. Figure 7 presents a general curve in which the dry fraction of the contact area was one coordinate and the fraction of burnout heat flux was the other. Information from references 33, 37, and 39 permits the construction of a general curve of this type. Fortunately, the type of heating surface employed in each of these investigations was similar (conductive glass). Surface tension has not been considered in developing figure 7.

The circles in figure 7 represent data obtained from reference 33 for heat flux, which are approximately 2, 3, and 4 percent of the critical value (the critical heat flux for water is taken as 5×10^5 Btu/(hr)(ft^2) (1.57×10^6 W/m^2). Figure 16(b) of reference 39 shows an instantaneous view of dry spots at a heat flux which is at 20 percent of burnout. The dry area is similar in shape and magnitude to that of the lower heat fluxes in reference 33. The square symbol in figure 7 is an estimate from figure 16(b) of reference 39. The authors of reference 37 observed that the dry-spot area fraction remained substantially constant up to 70 percent of the critical flux. Consequently, the portion of the curve in figure 7 for heat flux, which varies from 4 to 70 percent of the critical flux, is drawn with the percent dry spot as a constant.

The onset of burnout was described in references 37 and 39 as a highly transient state at the local burnout point where film boiling rapidly replaces multiple-bubble nucleate boiling. Thus, above 70 percent of the burnout flux, the fraction of dry area for a constant heat-flux surface grows asymptotically toward 1.

Contact angle. - Reference 31 presents contact-angle data for steam bubbles in water. The average contact angle was 30°. No published data were found for methanol; however, it is expected that the contact angle would be smaller because the surface tension of methanol is less than that of water. An estimated value of 20° was used in the calculations. High-speed motion pictures of ethanol (private communication with R. Siegel and E. G. Keshock) indicated that the contact area of the bubble could be approximated by a 20° contact angle.

The experimental information on the contact angle was obtained from isolated bubbles. It was assumed that large multiple bubbles could be considered to be agglomerates of single bubbles and that the same contact-angle information which was applied to the multiple bubbles could be applied to the single bubbles.

Pressure difference in evaporation. - Equation (4) contains a pressure-difference term $p_l - p_r$, where p_l was assumed to represent a saturation pressure corresponding to an average temperature of the microlayer during the bubble growth

$$T_{av} = \frac{T_w - T_{sat}}{2}$$

where T_{sat} is the saturation temperature at bulk conditions of liquid. This average temperature was chosen because figure 3 shows that the surface temperature under a bubble undergoes an almost linear drop during the early stage of the growth period when evaporation is significant. An arithmetic average is a good approximation to an average surface temperature, and the microlayer temperature must be related to the wall temperature.

The inherent sensitivity of the saturation-pressure value to the saturation temperature influences greatly the term $p_l - p_r$ in equation (4). The selection of p_l is an empiricism that can be judged on the reasonableness of the estimate of Q_{evap} obtained near the burnout condition. The numerical results (table V) indicate that the previously described method for selecting p_l is reasonable. The evaporative coefficient a in equation (4) was obtained from the literature (see table I, p. 9).

Surface of Boiling Preparation

This portion of the surface is assumed to be undergoing transient conduction while an area around a site is prepared for the birth of a bubble. The area in preparation is assumed to be equal to the statistical bubble area πr_b^2.

Equation (7) requires experimental information on the waiting period. The average waiting period can be computed form the statistical data of a boiling experiment in the following fashion. The ratio of the number of instantaneous bubbles n_{av} to the number

of bubble sites N of a surface (see table III, p. 21):

$$\frac{\tau_{gr}}{\tau_w + \tau_{gr}} = \frac{n_{av}}{N}$$

or

$$\frac{\tau_w}{\tau_w + \tau_{gr}} = 1 - \frac{n_{av}}{N} \tag{12}$$

Obtaining a numerical value for τ_w requires that a value be assigned to τ_{gr}. It is well known that the growth time for individual bubbles is a function of heat flux and subcooling. In figure 12 of reference 37, the dependence of growth time on heat flux is shown for carbon tetrachloride. The data encompass the entire nucleate-boiling regime from incipience to burnout. Herein, this dependency of growth time on heat flux for carbon tetrachloride (ref. 37) was generalized, and a curve of a normalized growth time, $\tau_{gr}/\tau_{gr,ref}$ was plotted as a function of the percent of the critical heat flux in figure 9. For the fluids considered, $\tau_{gr,ref}$ was assumed to be 10^{-2} second. This value is representative of much experimental data for water, but it is probably too large for methanol. The shaded region in figure 9 reflects the uncertainty in the values obtained for heat flux and bubble-growth times in the vicinity of the incipience point. No attempt was made to correct the bubble-growth times for subcooling effects.

For ease of calculation, the thermal properties inserted in equation (7) were taken at bulk conditions. Perhaps a more accurate selection would be to use film properties, but the result would not differ appreciably.

As pointed out previously in this report, the area of preparation A_{prep} is assumed to be related to the ratio τ_w/τ_{gr} and to the area of evaporation A_{evap}. At the higher heat-flux portion of the boiling curve, the areas of preparation and evaporation of multiple bubbles probably overlap. It was assumed in this model that no such overlap occurs. Equation (11) (and its restraint) is valid over the entire range of the nucleate-boiling heat flux. An inconsistency between the ratio of evaporative to preparation areas and the ratio of growth to waiting times appears in run 5 (table III) and is attributed to overlapping. For this near burnout run, τ_w/τ_{gr} is much greater than A_{evap}/A_{prep} or $\varphi/(1 - \Phi)$ and thus violates the restraint of equation (11) $\left[\Phi + (\tau_w/\tau_{gr})(\Phi) \leq 1)\right]$. For the burnout and near-burnout runs of reference 39, the restraint of equation (11) was not violated. No statistical information on bubble sites and population was available; therefore, τ_w/τ_{gr} was estimated from information on the instantaneous areas of evaporation and from equation (11) with the restraint applied.

Nonboiling Surface

The estimation of the turbulent free-convection heat flux was discussed in the previous section of this appendix. The area undergoing turbulent free convection is assumed to be that surface which is not participating in some aspect of the ebullition process or is not directly linked to the bubble growth, as is the case for the area of influence (enhanced turbulent convection).

For some of the computations with methanol, no surface area was left for the free-convection component because the entire surface was engaged in the boiling mechanisms. In fact, for run 5, so much of the surface was engaged in supporting ebullition that no enhanced or free-convection areas were available. What was done in these cases was to start the computation with the evaporative area. The residue of area left to other mechanisms was taken in the order of transient conduction first and then enhanced convection.

Justification for the assumption of the overcrowding of a surface by the boiling mechanisms can be seen in reference 35, wherein it was noted that the spacing between active sites was reduced rapidly as the heat flux was increased.

Sample Calculation

The following sample calculation presents the estimates of each contribution to the overall heat flux for nucleate boiling in water. Similar calculations were made for methanol.

The following input data were inserted in the heat flux equations of the model for water:

(1) Properties of water (including evaporation coefficient):

$$T_{sat} = 212^{\circ} \text{ F}$$

$$P = 1 \text{ atm}$$

$$\alpha = 6.5 \times 10^{-3} \text{ ft}^2/\text{hr}$$

$$k = 0.39 \text{ Btu/(hr)(ft)}(^{\circ}\text{R})$$

$$\lambda = 970 \text{ Btu/lb}$$

$$a = 0.04$$

(2) Statistical boiling information:

From references 11 and 38, $T_w - T_b = 27^o$ F and $T_w = 225^o$ F. Since $\tau_{gr}/(\tau_{gr} + \tau_w) = 0.16$, and $\tau_{gr} = 0.01$, $\tau_w + \tau_{gr} = 0.06$ second; thus, $\tau_w = 0.05$ second.
Evaporation contribution (first term of eq. (10)):

$$q_{evap} = a\lambda(p_l - p_r)\left(\frac{g_c M}{2\pi R T_{sat}}\right)^{1/2}$$

where p_l is the saturation pressure at

$$T = \frac{T_w + T_{sat}}{2} = 218.5^o \text{ F}$$

$$p_l = 16.8 \text{ psia}$$

$$q_{evap} = (0.04)(970)(16.8 - 14.7)144\left(\frac{18 \times 32.2}{2\pi \times 1544 \times 672}\right)^{1/2} 3600$$

$$= 400\ 000 \text{ Btu/(hr)(ft}^2\text{)}$$

Conduction contribution (third term of eq. (10)):

$$q_{cond} = 2k(T_w - T_b)\left(\frac{1}{\sqrt{\tau_w}}\,\frac{1}{\sqrt{\pi\alpha}}\right)$$

$$= 2\times 0.39(27)\left(\frac{1}{\sqrt{14\times 10^{-6}}}\,\frac{\sqrt{10^3}}{6.5\,\pi}\right)$$

$$= 34\ 500 \text{ Btu/(hr)(ft}^2\text{)}$$

Convection contribution:

Rather than computing the free-convection contribution, recourse is made to reference 36 where indications of the free-convection heat flux were measured.

$\bar{q}_{enh\ conv} = 11\ 000 \times 1.5 = 16\ 500$ Btu/(hr)(ft^2) (second term of eq. (10)):

The multiplier 1.5 in $\bar{q}_{enh\ conv}$ is the enhancement factor.

$\bar{q}_{\text{free conv}} = 11\ 000$ Btu/(hr)(ft^2) (fourth term of eq. (10)):

Area-weighted contribution:

$$\frac{Q_{evap}}{A_h} = q_{evap}\frac{A_{evap}}{A_h}$$

$$= 400\ 000\left[\Phi(1 - Dr)\sin^2\beta\right]$$

For

$$\beta = 30^o$$

and

$$Dr = 0.15$$

$$\frac{Q_{evap}}{A_h} = (400\ 000)(0.0173)$$

$$= 7000 \qquad \text{(a)}$$

$$\frac{Q_{cond}}{A_h} = q_{cond}\frac{A_{cond}}{A_h}$$

$$= 34\ 500\left(\Phi\frac{\tau_w}{\tau_{gr}}\right)$$

$$= 45\ 500\ (0.436)$$

$$= 14\ 900 \qquad \text{(b)}$$

$$\frac{Q_{enh\ conv}}{A_h} = q_{enh\ conv} \frac{A_{enh\ conv}}{A_h}$$

$$= 16\ 500 \left[\Phi(4 - \sin^2\beta)\right]$$

$$= 16\ 500\ (0.312) = 5100 \qquad \text{(c)}$$

$$\frac{Q_{conv}}{A_h} = q_{conv} \frac{A_{conv}}{A_h}$$

$$= 11\ 000\left[1 - (A_{evap} + A_{cond} + A_{enh\ conv})\right] \qquad \text{(d)}$$

$$= 11\ 000\ (0.235)$$

$$= 2600 \qquad \text{(d)}$$

The summation of all the contributions is

$$\sum \frac{Q}{A_h} = 29\ 600\ \text{Btu/(hr)(ft}^2\text{)}$$

REFERENCES

1. Bankoff, S. G.: On the Mechanism of Subcooled Nucleate Boiling. AIChE Chem. Eng. Progr. Symp. Ser., vol. 57, no. 32, 1961, pp. 156-172.

2. Engelberg-Forster, Kurt; and Greif, R.: Heat Transfer to a Boiling Liquid - Mechanism and Correlations. J. Heat Transfer, vol. 81, no. 1, Feb. 1959, pp. 43-53.

3. Hendricks, Robert C.; and Sharp, Robert R.: Initiation of Cooling Due to Bubble Growth on a Heating Surface. NASA TN D-2290, 1964.

4. Zuber, Novak; and Fried, Erwin: Two-Phase Flow and Boiling Heat Transfer to Cryogenic Liquids. ARS J., vol. 32, no. 9, Sept. 1962, pp. 1332-1341.

5. Levy, S.: Generalized Correlation of Boiling Heat Transfer. J. Heat Transfer, vol. 81, no. 1, Feb. 1959, pp. 37-42.

6. Snyder, N. R.; and Edwards, D. K.: Post Conference Comments. Summary of Conference on Bubble Dynamics and Boiling Heat Transfer Held at the Jet Propulsion Laboratory, June 14 and 15, 1956. S. G. Bankoff, W. J. Colahan, Jr., and D. R. Bartz, eds. Memo No. 20-137, Jet Propulsion Lab., California Inst. Tech., Dec. 10, 1956, p. 38.

7. Moore, Franklin D.; and Mesler, Russell B.: The Measurement of Rapid Surface Temperature Fluctuations During Nucleate Boiling of Water. AIChE J., vol. 7, no. 4, Dec. 1961, pp. 620-624.

8. Plesset, Milton S.: Note on the Flow of Vapor Between Liquid Surfaces. J. Chem. Phys., vol. 20, no. 5, May 1952, pp. 790-793.

9. Bankoff, S. G.: A Note on Latent Heat Transport in Nucleate Boiling. AIChE J., vol. 8, no. 1, Mar. 1962, pp. 63-65.

10. Kast, W.: Importance of Nucleation Activation and Nonstationary Heat Transp for the Heat Transfer in Nucleate Boiling and Dropwise Condensation. Chem.-Ingr.-Tech., vol. 36, no. 9, Sept. 1964, pp. 933-940.

11. Raben, Irwin A.; Beaubouef, Richard T.; Commerford, G. E.: A Study of Heat Transfer in Nucleate Pool Boiling of Water at Low Pressure. AIChE Chem. Eng. Progr. Symp. Ser., vol. 61, no. 57, 1965, pp. 249-257.

12. Ruckenstein, E.: Remarks on Nucleate Boiling Heat Transfer From a Horizontal Surface. Int. J. Heat Transfer, vol. 9, no. 3, Mar. 1966, pp. 229-237.

13. Torikai, K.; and Yamazaki, T.: Photographical Study for Boiling Heat Transfer Mechanism. Proceedings of the Third International Heat Transfer Conference, Chicago, Illinois, ASME-AIChE, Aug. 1966, vol. 3, pp. 239-244.

14. Hsu, Yih-Yun; and Graham, Robert W.: An Analytical and Experimental Study of Thermal Boundary Layer and Ebullition Cycle in Nucleate Boiling. NASA TN D-594, 1961.

15. Gaertner, R. F.; and Westwater, J. W.: Population of Active Sites in Nucleate Boiling Heat Transfer. AIChE Chem. Eng. Progr. Symp. Ser., vol. 56, no. 30, 1960, pp. 39-48.

16. Graham, Robert W.; Hendricks, Robert C.; and Ehlers, Robert C.: Analytical and Experimental Study of Pool Heating of Liquid Hydrogen Over a Range of Accelerations. NASA TN D-1883, 1965.

17. Holt, V. E.; and Grosh, R. J.: Free Convection Heat Transfer Up to Near-Critical Conditions. Nucleonics, vol. 21, no. 8, Aug. 1963, pp. 122-125.

18. Mixon, F. O., Jr.; Chon, Wang Yong; and Beatty, K. O., Jr.: The Effect of Electrolytic Gas Evolution on Heat Transfer. AIChE Chem. Eng. Progr. Symp. Ser., vol. 56, no. 30, 1960, pp. 75-81.

19. Gunther, Fred C.; and Kreith, Frank: Photographic Study of Bubble Formation in Heat Transfer To Subcooled Water. Prog. Rept. 4-120, Jet Propulsion Lab., Calibronia Ins.. Tech., Mar. 9, 1959.

20. Marcus, B. D.; and Dropkin, D.: Measured Temperature Profiles Within the Superheated Boundary Layer Above A Horizontal Surface in Saturated Nucleate Pool Boiling of Water. J. Heat Transfer, vol. 87, no. 3, Aug. 1965, pp. 333-341.

21. Graham, Robert W.: Experimental Observations of Transient Boiling of Subcooled Water and Alcohol on a Horizontal Surface. NASA TN D-2507, 1965.

22. Hsu, Y. Y.: On the Size Range of Active Nucleation Cavities on a Heating Surface. J. Heat Transfer, vol. 84, no. 3, Aug. 1962, pp. 207-216.

23. Kennard, Earle H.: Kinetic Theory of Gases. McGraw-Hill Book Co., Inc., 1938, pp. 60-74.

24. Wyllie, G.: Evaporation and Surface Structure of Liquids. Roy. Soc. Proc., ser. A, vol. 197, no. 1050, June 22, 1949, pp. 383-395.

25. Paul, B.: Compilation of Evaporation Coefficients. ARS J., vol. 32, no. 9, Sept. 1962, pp. 1321-1328.

26. Chu, H. D.; Delaney, L. J.; and Eagleton, L. C.: The Rate of Vaporization of Deuterium Oxide. Chem. Eng. Science, vol. 20, no. 6, June 1965, pp. 601-605.

27. Delaney, L. J.; Psaltis, N. J.; and Eagleton, L. C.: The Rate of Vaporization of Methanol. Chem. Eng. Science, vol. 20, no. 6, June 1965, pp. 607-610.

28. Marcus, Bruce D.: Experiments on the Mechanism of Saturated Nucleate Pool Boiling Heat Transfer. Ph.D. Thesis, Cornell Univ., 1963.

29. Bonnet, C.; Macke, E.; and Morin, R.: Visualization of Bubble Formation at Atmospheric Pressure and Related Measurement of the Wall Temperature Variations. Rep. No. EUR 1622. e, European Atomic Energy Community, Apr. 1965.

30. Cooper, M. G.; and Lloyd, A. B.: Transient Local Heat Flux in Nucleate Boiling. Proceedings of the Third International Heat Transfer Conference, Chicago, Ill., ASME, AIChE, Aug. 1966, vol. 3, pp. 193-203.

31. Bankoff, S. G.; and Mason, J. P.: Heat Transfer from the Surface of a Steam Bubble in Turbulent Subcooled Liquid Stream. AIChE J., vol. 8, no. 1, Mar. 1962, pp. 30-33.

32. Hospeti, Narayan B.; and Mesler, Russell B.: Deposits Formed Beneath Bubbles During Nucleate Boiling of Radioactive Calcium Sulfate Solutions. AIChE J., vol. 11, no. 4, July 1965, pp. 662-665.

33. Sharp, Robert R.: The Nature of Liquid Film Evaporation During Nucleate Boiling. NASA TN D-1997, 1964.

34. Siegel, R.; and Keshock E. G.: Effects of Reduced Gravity on Nucleate Boiling Bubble Dynamics in Saturated Water. AIChE J., vol. 10, no. 4, July 1964, pp. 509-517.

35. Buehl, W. M.; and Westwater, J. W.: Bubble Growth by Dissolution: Influence of Contact Angle. AIChE J., vol. 12, no. 3, May 1966, pp. 571-576.

36. Graham, Robert W.; and Hendricks, Robert C.: A Study of the Effect of Multi-g Accelerations on Nucleate-Boiling Ebullition. NASA TN D-1196, 1963.

37. Kirby, D. B.; and Westwater, J. W.: Bubble and Vapor Behavior on a Heated Horizontal Plate During Pool Boiling Near Burnout. AIChE Chem. Eng. Progr. Symp. Ser., vol. 61, no. 57, 1965, pp. 238-248.

38. Hsu, Yih-Yun: Gradual Transition of Nucleate Boiling From Discrete-Bubble Regime to Multibubble Regime. NASA TN D-2564, 1964.

39. Torikai, Kinichi; and Yamazaki, Toshi: The Contact Area of Boiling Bubbles on the Heating Surface. J.S.M.E. Bulletin, vol. 8, no. 32, 1965, p. 660-669.

40. Zuber, Novak: Nucleate Boiling. The Region of Isolated Bubbles and the Similarity with Natural Convection. Int. J. Heat Mass Transfer, vol. 6, no. 1, Jan. 1963, 53-78.

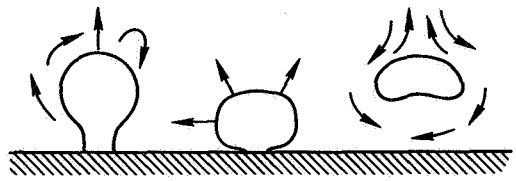

(a) Bubble agitation.

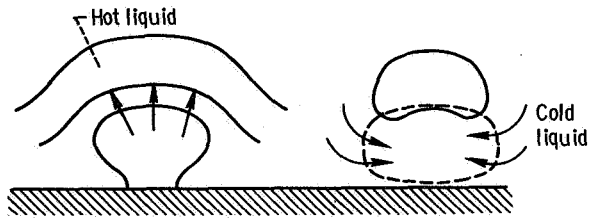

(b) Vapor-liquid exchange.

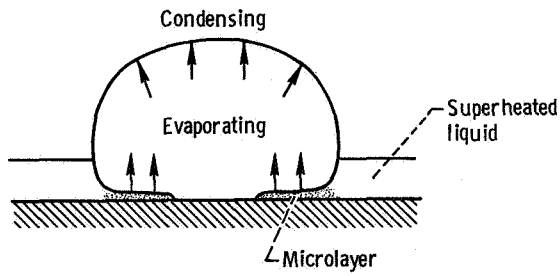

(c) Evaporation.

Figure 1. - Schematic diagram of nucleate boiling models.

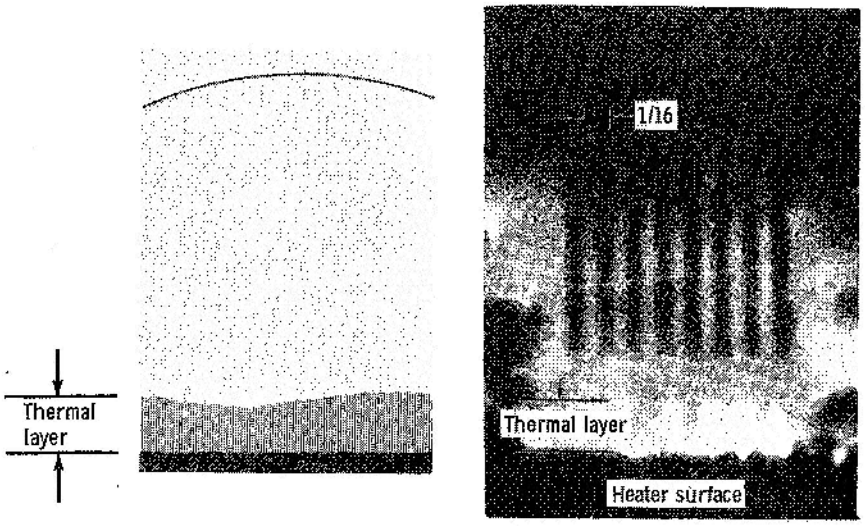

Established thermal layer

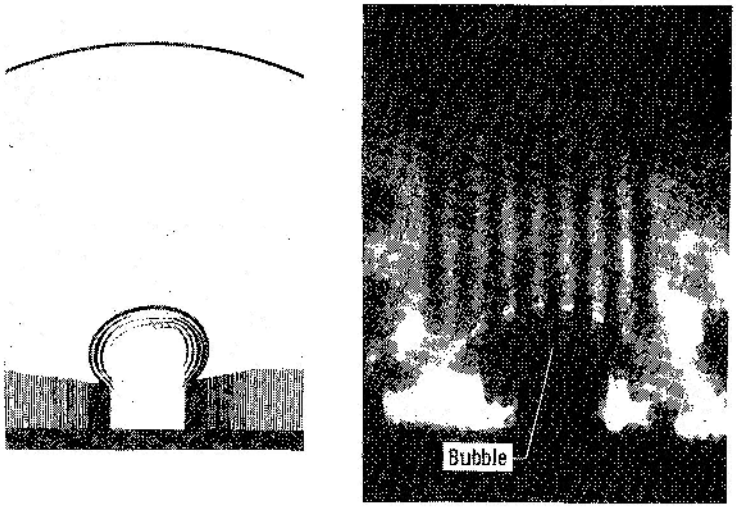

Bubble growth period

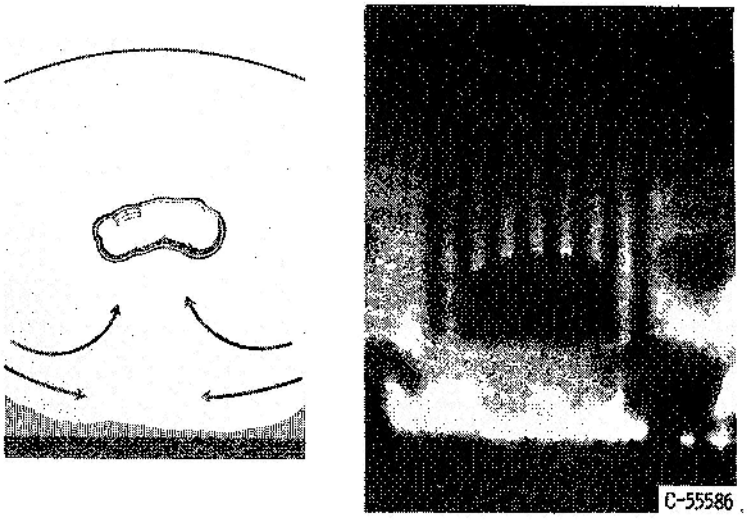

Destruction of thermal layer

Figure 2. - Principal stages in life of thermal layer.

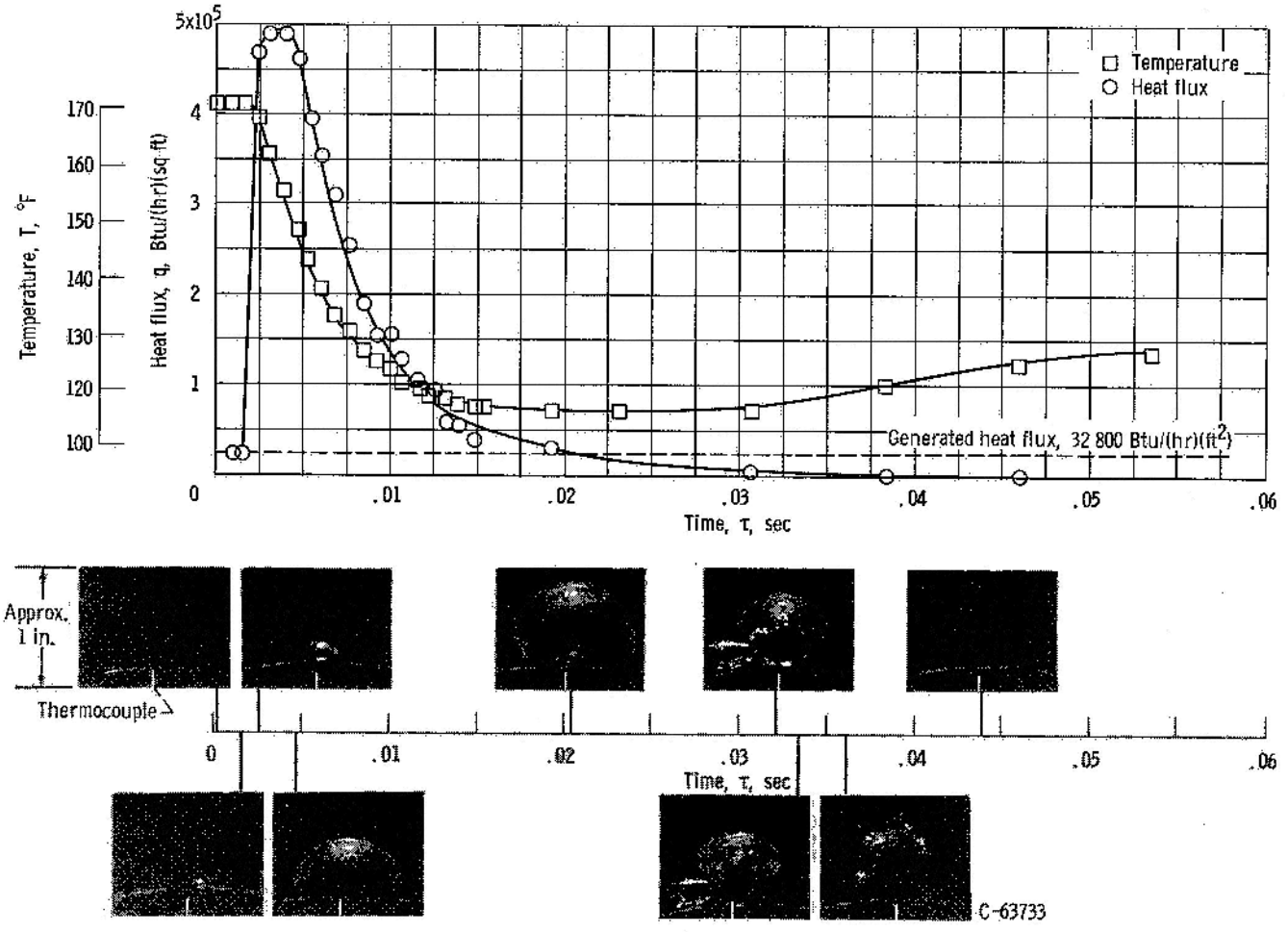

Figure 3. - Temperature and heat flux beneath growing bubble. Saturation temperature, 95° F; liquid bulk temperature, 84° F; liquid, water; reduced pressure.

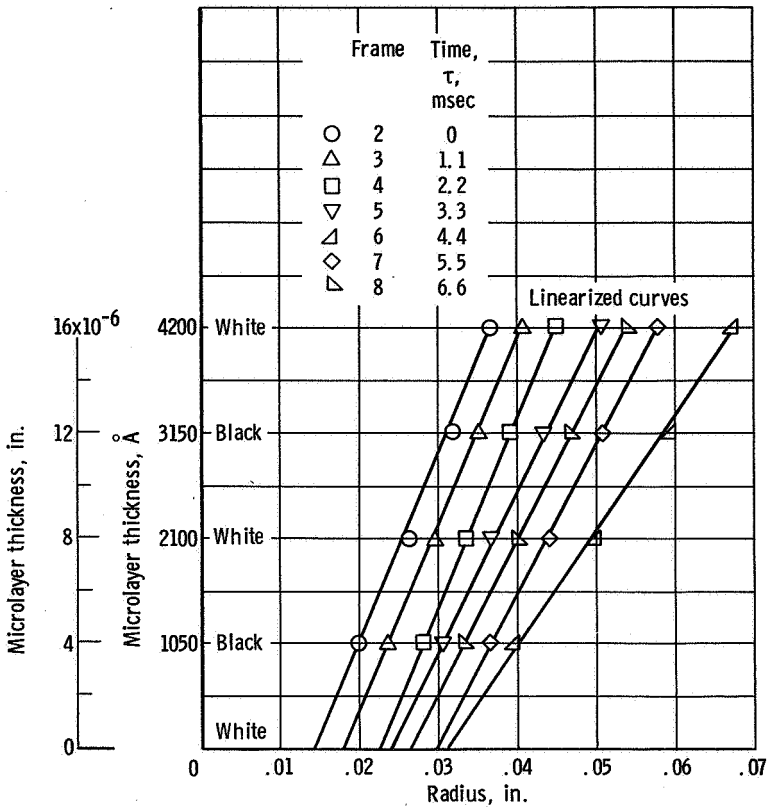

Figure 4. - Microlayer thickness as function of radius.

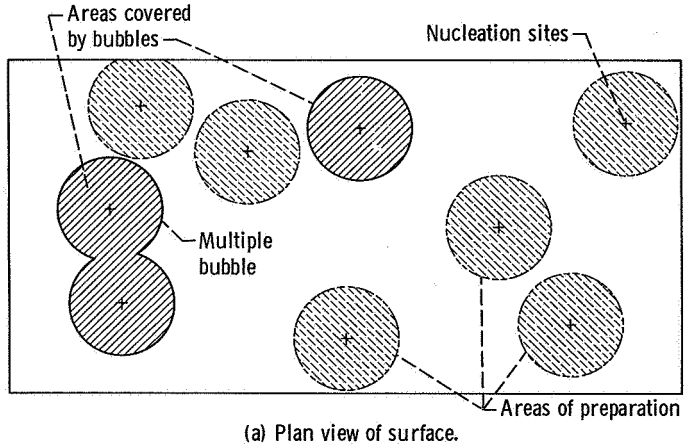

(a) Plan view of surface.

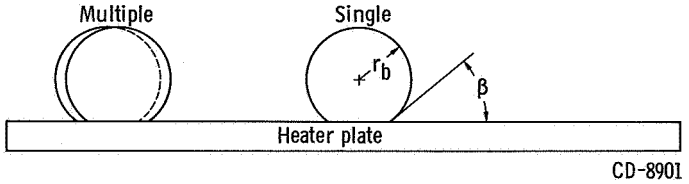

CD-8901

(b) Profile view of statistical bubbles.

Figure 5. - Instantaneous representation of nucleate-boiling surface. (The waiting period is equal to twice the growth period.)

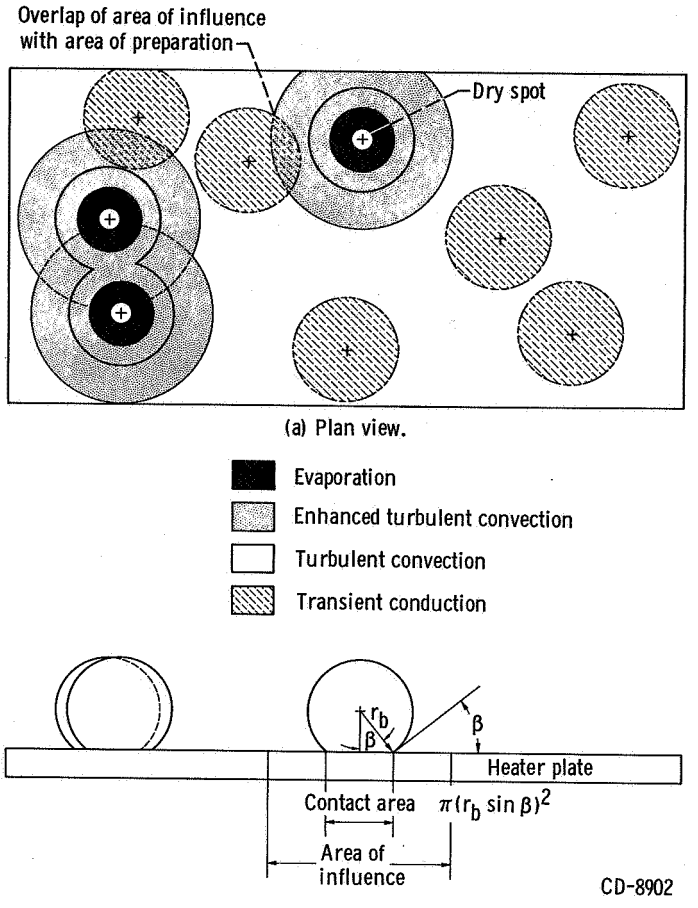

Figure 6. - Distribution of heat-transfer mechanisms over nucleate-boiling surface.

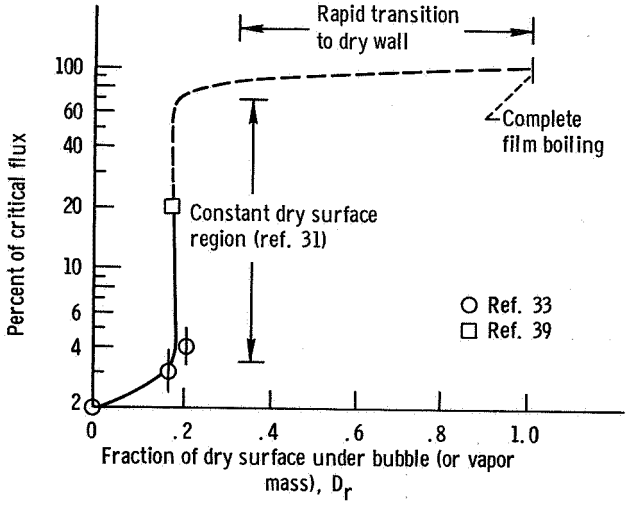

Figure 7. - Fraction of dry surface under bubble as function of dimensionless heat flux.

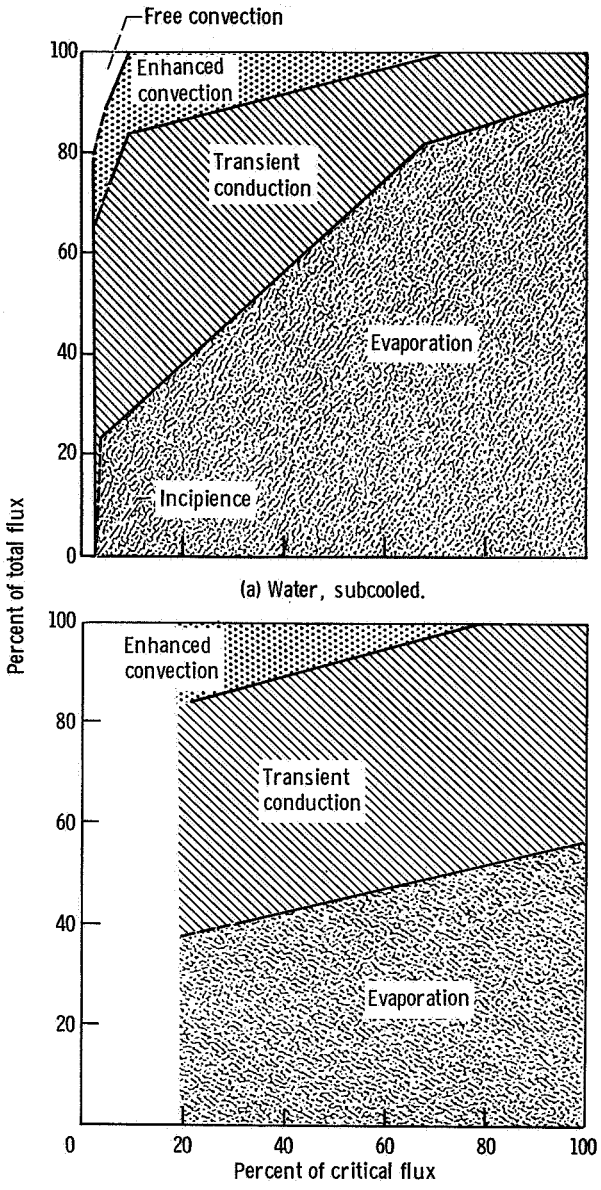

Figure 8. - Relative contributions of heat-transfer mechanisms over range of average heat flux.

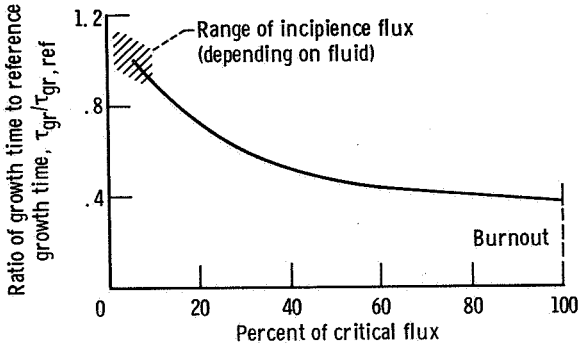

Figure 9. - Growth time of bubbles as function of percent of critical heat flux. (Based on fig. 12 from ref. 37.)

Motion picture C-252 is available on loan. Requests will be filled in the order received. You will be notified of the approximate date scheduled.

The film (16 mm, 7 min, color, sound) shows actual high-speed motion pictures of evaporative microlayers underneath growing bubbles. Reflective images and Newton rings of the microlayer are presented as evidence of the existence of the microlayer.

Motion picture C-252 is available on request to

Chief, Technical Information Division (5-5)
National Aeronautics and Space Administration
Lewis Research Center
21000 Brookpark Road
Cleveland, Ohio 44135

CUT

Date _____

Please send, on loan, copy of Motion Picture C-252 to

_____

Name of organization

_____

Street number

_____

City and State Zip code

Attention: Mr. _____

9/5/67

"The aeronautical and space activities of the United States shall be conducted so as to contribute . . . to the expansion of human knowledge of phenomena in the atmosphere and space. The Administration shall provide for the widest practicable and appropriate dissemination of information concerning its activities and the results thereof."

—NATIONAL AERONAUTICS AND SPACE ACT OF 1958

NASA SCIENTIFIC AND TECHNICAL PUBLICATIONS

TECHNICAL REPORTS: Scientific and technical information considered important, complete, and a lasting contribution to existing knowledge.

TECHNICAL NOTES: Information less broad in scope but nevertheless of importance as a contribution to existing knowledge.

TECHNICAL MEMORANDUMS: Information receiving limited distribution because of preliminary data, security classification, or other reasons.

CONTRACTOR REPORTS: Scientific and technical information generated under a NASA contract or grant and considered an important contribution to existing knowledge.

TECHNICAL TRANSLATIONS: Information published in a foreign language considered to merit NASA distribution in English.

SPECIAL PUBLICATIONS: Information derived from or of value to NASA activities. Publications include conference proceedings, monographs, data compilations, handbooks, sourcebooks, and special bibliographies.

TECHNOLOGY UTILIZATION PUBLICATIONS: Information on technology used by NASA that may be of particular interest in commercial and other non-aerospace applications. Publications include Tech Briefs, Technology Utilization Reports and Notes, and Technology Surveys.

Details on the availability of these publications may be obtained from:

SCIENTIFIC AND TECHNICAL INFORMATION DIVISION

NATIONAL AERONAUTICS AND SPACE ADMINISTRATION

Washington, D.C. 20546